

Pulse EPR Measurements of Intramolecular Distances in a TOPP-Labeled Transmembrane Peptide in Lipids

Karin Halbmaier,¹ Janine Wegner,² Ulf Diederichsen,² and Marina Bennati^{1,2,*}

¹Electron Spin Resonance Spectroscopy, Max Planck Institute for Biophysical Chemistry, Göttingen, Germany; and ²Institute for Organic and Biomolecular Chemistry, Georg-August-University, Göttingen, Germany

ABSTRACT We present the performance of nanometer-range pulse electron paramagnetic resonance distance measurements (pulsed electron-electron double resonance/double electron-electron resonance, PELDOR/DEER) on a transmembrane WALP24 peptide labeled with the semirigid unnatural amino acid 4-(3,3,5,5-tetra-methyl-2,6-dioxo-4-oxylpiperazin-1-yl)-l-phenylglycine (TOPP). Distances reported by the TOPP label are compared to the ones reported by the more standard MTSSL spin label, commonly employed in protein studies. Using high-power pulse electron paramagnetic resonance spectroscopy at Q-band frequencies (34 GHz), we show that in contrast to MTSSL, our label reports one-peak, sharp ($\Delta r \leq 0.4$ nm) intramolecular distances. Orientational selectivity is not observed. When spin-labeled WALP24 was inserted in two representative lipid bilayers with different bilayer thickness, i.e., DMPC and POPC, the intramolecular distance reported by TOPP did not change with the bilayer environment. In contrast, the distance measured with MTSSL was strongly affected by the hydrophobic thickness of the lipid. The results demonstrate that the TOPP label is well suited to study the intrinsic structure of peptides immersed in lipids.

Understanding the functionality and organization of peptides and proteins in biological membranes requires knowledge of their molecular structures and conformational dynamics. Crystallization of membrane proteins or protein complexes is still challenging and conformations found in the crystallized state may not represent the biologically active species. Therefore, development of other complementary spectroscopic methods like nuclear magnetic resonance spectroscopy or electron paramagnetic resonance techniques (EPR) becomes essential (1,2). Pulsed electron-electron double resonance (PELDOR) or double electron-electron resonance (DEER) is an EPR-based method that emerged as a powerful tool to measure interspin distances and orientations in biomolecules in a range between ~2 and 10 nm (3–5). The method detects the magnetic dipole-dipole interaction between two paramagnetic centers, usually nitroxide radicals that are site-selectively inserted in biomolecules either via mutagenesis or more sophisticated methods such as ligation or synthetically generated peptides, or via *in vivo* introduction of unnatural

amino acids (6,7). In samples of peptides or proteins, intermolecular interactions can lead to high local concentrations of spin labels, which in turn reduce transverse spin relaxation and the detectable signal (8). In this case, the sensitivity of the PELDOR experiment becomes an issue. Performing distance measurements at Q-band frequencies and fields (34 GHz/1.2 T), a condition that is superior in terms of sensitivity over X-band (0.34 T, 9 GHz), becomes an essential advantage (9). Moreover, in lipid bilayers, the flexibility of standard labels such as MTSSL combined with nonhomogeneous distribution of peptides, leads to complex distance distributions. To overcome this issue, nitroxide labels with reduced mobility like RX and TOAC have been proposed in Schreier et al. (10) and Fleissner et al. (11). Although they have great potential, RX requires two cysteine mutations per spin label and TOAC is an achiral C α -bis substituted amino acid with impact on the peptide secondary structure. The latter is known to adopt helical torsion angle, rendering it well suited for investigating β -bends and α -helices while introduction into other structural motifs might cause structural distortions (10,12,13). As a potential alternative, we have previously introduced a semirigid spin label for peptide studies, called 4-(3,3,5,5-tetra-methyl-2,6-dioxo-4-oxylpiperazin-1-yl)-l-phenylglycine (TOPP) (Fig. 1, inset), based on an unnatural amino acid, in which the

Submitted August 4, 2016, and accepted for publication October 19, 2016.

*Correspondence: marina.bennati@mpibpc.mpg.de

Editor: David Cafiso.

<http://dx.doi.org/10.1016/j.bpj.2016.10.022>

© 2016 Biophysical Society.

This is an open access article under the CC BY license (<http://creativecommons.org/licenses/by/4.0/>).

Halbmaier et al.

NH₂-KW~~WL~~-X-LALALALALALALA-X-AWWANH₂

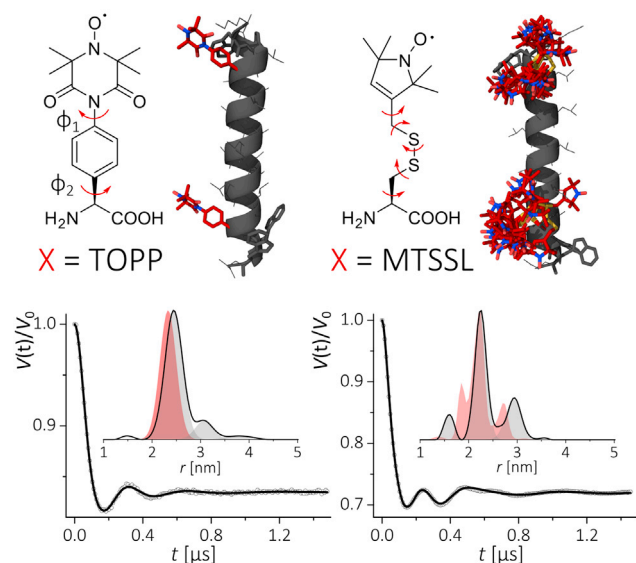


FIGURE 1 (Top) The peptide sequence of WALP24 showing the positions (X), at which the spin labels have been inserted. (Center) Chemical structure of the TOPP (left) and MTSSL (right) spin labels. Structures were modeled as explained in the Supporting Material. (Bottom) PELDOR experiments on WALP24 in methanol. Background-corrected PELDOR time traces (dots) and fits using Tikhonov regularization (DeerAnalysis) (26) (lines) for WALP24-TOPP (left) and WALP24-MTSSL (right). Experimental and modeled distance distributions are shown in comparison (filled line and area). Original traces are displayed in Fig. S3.

position of the spin bearing NO-group is fixed in space (7). We have reported the performance of TOPP in distance measurements in solution and for measurements of relative orientations with high-field EPR (14). Here we present the performance of TOPP as compared to the standard MTSSL label in reporting intramolecular distances in lipid environment.

As a model system for a comparative study, we have employed a WALP model peptide, which is composed of a hydrophobic stretch of alternating leucines and alanines flanked at both ends by a pair of tryptophans (15). The latter provide anchoring in the headgroup area of the membrane and are expected to influence the orientation of the peptide helix as a transmembrane segment. The rationale for the choice of WALP were the recent reports on the stability and good adaptation of WALP into lipid bilayers in conjunction with nitroxide spin labels and with more bulky labels such as lanthanide chelates (16,17). Spin-labeled WALP24 peptides were synthesized by solid-phase peptide synthesis as described in Supporting Material. The amino acid sequence is shown in Fig. 1 (top) together with the labeling positions within the transmembrane domain of the peptide. While MTSSL was attached postsynthetically to a cysteine mutation at the selected label position, the TOPP amino acid was introduced by manual solid-phase peptide synthesis un-

der conditions preventing racemization. Preservation of an α -helical structure of spin-labeled peptides in all environments used in the EPR experiments was confirmed by circular dichroism spectroscopy (Fig. S2). All distance measurements were performed using the standard four-pulse PELDOR sequence at Q-band frequencies with a high-power 170 W TWT amplifier (Supporting Material). Samples were of ~ 20 – 30 μ M peptide bulk concentration in solvent or deuterated lipids.

To evaluate the capability of the TOPP label to report on intramolecular distances, we have first investigated a doubly labeled WALP24 peptide dissolved in methanol. In Fig. 1, typical PELDOR dipolar traces are shown that reflect the dipolar interaction between the two labels and their interspin distance. Dipolar oscillations are well visible in the traces recorded with both types of labels. However, inspection of the WALP24-MTSSL trace reveals the contribution of more than one dipolar frequency. Fourier transformation confirms the superposition of at least two Pake patterns in the latter case (Fig. S3). Instead, the trace recorded on the TOPP-labeled peptide shows one main frequency component. Analysis reveals a single-peak distance distribution for TOPP as compared to a more complex distribution with MTSSL. The observed distances and distributions could be well rationalized by simple molecular modeling as explained in Fig. S4 (18,19). The predicted peak distance for the TOPP-labeled peptide (averaged among the O-O, N-O, and N-N distances) of $r = 2.33$ nm is in close agreement with the peak distance (most probable distance) from the experiment of $r = (2.45 \pm 0.05)$ nm and a distribution Δr (peak half-width at half-height) of 0.2 nm. The small shift between the modeled and experimental peak distance ($\Delta \approx 0.1$ nm) actually exceeds the estimated experimental error (Fig. S3) and is likely due to simplicity of the structural modeling. The modeling clearly predicts that rotamers of MTSSL are responsible for the distance distribution with multiple peaks (Fig. 1). The results indicate that detailed interpretation of interspin distances using MTSSL labels becomes more difficult if distances arising from different conformations of the biomolecule might superimpose upon distances from MTSSL rotamers. Because the TOPP label is quasirigid, attention must be paid to whether the observed intramolecular distances and distributions are affected by orientation selection (14). To examine this, we have recorded the traces under the conditions of Fig. 1 but changing the resonance positions of detecting frequencies in the EPR line. A comparison of the resulting traces (Figs. S5–S7) reveals that there is no dependence of the dipolar frequency on the experimental setup, thus no orientation selection is observed.

In a subsequent step, we have investigated the spin-labeled WALP24 peptide in two different representative lipids, DMPC and POPC. The hydrophobic length of WALP24 matches well the hydrophobic thickness of POPC ($r \approx 2.7$ nm) but does not match the hydrophobic thickness of DMPC ($r \approx 2.3$ nm), as sketched in Fig. 2.

Therefore, these two lipids appeared as suited model systems to compare the capability of the labels to report on peptide structure in different lipid environments. To optimize the sample preparation for lipid studies, first an extensive study on WALP24-MTSSL in DMPC was performed. Different peptide/lipid values from 1:250 up to 1:3000 were tested to qualitatively monitor possible aggregation effects (Fig. S8). Aggregation of the spin-labeled peptide increases the number of spins participating in the PELDOR experiment, a fact that is manifested in an increasing modulation depth as well as in a faster spin-spin relaxation time T_2 (20,21). We have observed that for the ratio of 1:250 the T_2 relaxation time (Fig. S9) and the background decay of the PELDOR signal (Fig. S8) were both drastically reduced. For a peptide/lipid ratio of 1:1500, T_2 was shorter (Fig. S9) and the modulation depth increased (Fig. S8) as compared to the solution state, suggesting the onset of some aggregation. Therefore, to minimize intermolecular contributions, all distance measurements were performed at ratios at \sim 1:3000 or even lower. Sample preparation was further optimized by using deuterated lipids (D31-POPC, D54-DMPC; Fig. 2) permitting us to prolong electron spin relaxation times. Fig. 2 displays a comparison of PELDOR traces for TOPP- and MTSSL-WALP24 in DMPC and POPC. As the most significant result, we have found that the two

spin labels report significantly different distances. The peak distance between the TOPP labels does not show much dependence on the lipid environment within the experimental error, except for a slightly larger distribution up to $\Delta r = \pm 0.4$ nm in lipids as compared to methanol solution.

The result indicates that the peptide maintains its conformation in the two lipids and, at the same time, that TOPP is capable to report on the intrinsic peptide conformation. In contrast, the more flexible MTSSL label reports broad distance distributions. It is striking that the peak distances correspond to the hydrophobic thicknesses of the corresponding lipid. It has been reported that, due to their hydrophobicity, nitroxide spin labels insert into lipids and have a tendency to move to the interface region between the lipids tails and headgroups (22,23). Thus, flexibility of MTSSL allows for adapting to the membrane thickness resulting in loss of information about the internal peptide structure. It has been proposed that tryptophan anchors can influence bilayer thickness (24), making the adaption of the bilayer one reasonable mechanism to react on a mismatch condition. However, these results with WALP24-MTSSL instead point to peptide tilting as an alternative adaptation mechanism that would not alter the interspin distance (2). A rigid label like TOPP will be ideally suited for the investigation of

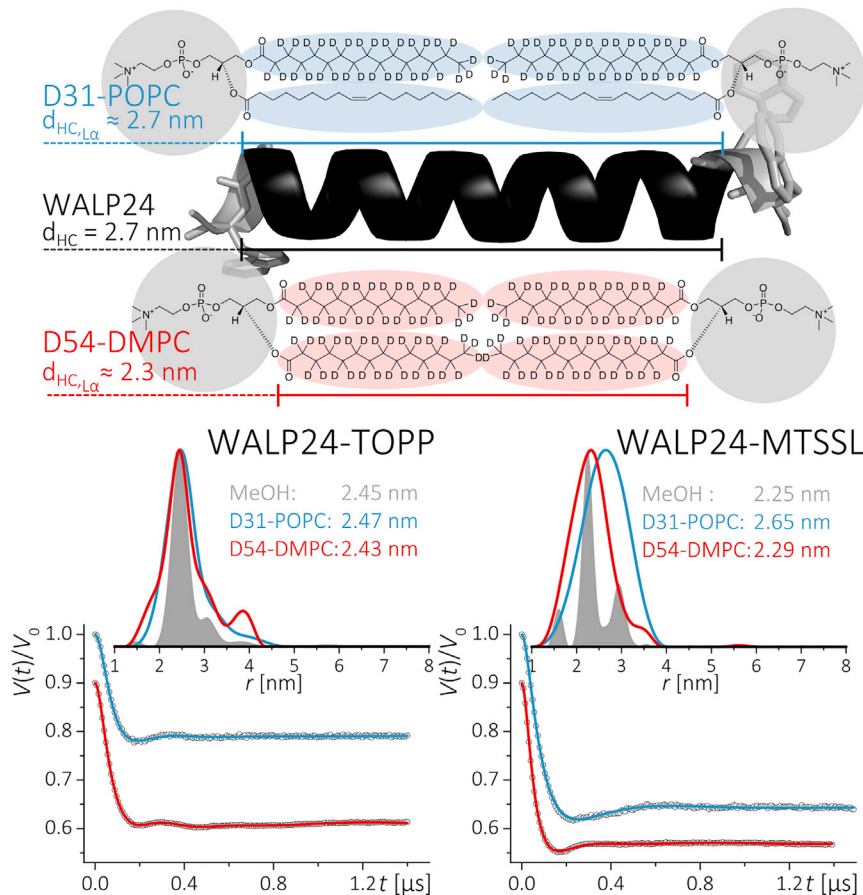


FIGURE 2 (Top) Chemical structure and schematic representation of the deuterated phospholipids D54-DMPC (14:0₂-d54 PC) and D31-POPC (16:0-d31-18:1 PC) used in this study with their hydrophobic thickness, as compared to the length of WALP24. **(Bottom)** PELDOR experiments of TOPP- (left) and MTSSL-labeled (right) WALP24 in different environments. Comparison of dipolar traces after background subtraction and distance distribution obtained from fits using Tikhonov regularization (DeerAnalysis). Differences in modulation depth are due to labeling efficiency. Original traces are displayed in Fig. S10.

Halbmaier et al.

the peptide tilt angles by PELDOR spectroscopy in an aligned membrane (25). Overall, this study demonstrates that the TOPP label is well suited for high-resolution measurements of interspin distances in transmembrane peptides.

SUPPORTING MATERIAL

Supporting Materials and Methods and ten figures are available at [http://www.biophysj.org/biophysj/supplemental/S0006-3495\(16\)30949-3](http://www.biophysj.org/biophysj/supplemental/S0006-3495(16)30949-3).

AUTHOR CONTRIBUTIONS

K.H. designed, performed, and analyzed EPR experiments; J.W. designed and performed peptide synthesis and characterization; M.B. helped with designing EPR experiments and wrote the article; and U.D. helped with designing peptide experiments and wrote the article.

ACKNOWLEDGMENTS

We thank B. Angerstein for help with preparation of lipid samples.

We acknowledge financial support from the Deutsche Forschungsgemeinschaft (DFG) collaborative research program SFB803 (project A2) and from the Max Planck Society.

REFERENCES

1. Sun, S., C. I. Neufeld, ..., Q. Xu. 2015. Chapter 17: Biophysical methods for the studies of protein-lipid/surfactant interactions. *In Recent Progress in Colloid and Surface Chemistry with Biological Applications*, ACS Symposium Series, Vol. 1215. American Chemical Society, Washington, DC, pp. 355–375.
2. Holt, A., and J. A. Killian. 2010. Orientation and dynamics of transmembrane peptides: the power of simple models. *Eur. Biophys. J.* 39:609–621.
3. Schiemann, O., and T. F. Prisner. 2007. Long-range distance determinations in biomacromolecules by EPR spectroscopy. *Q. Rev. Biophys.* 40:1–53.
4. Jeschke, G. 2012. DEER distance measurements on proteins. *Annu. Rev. Phys. Chem.* 63:419–446.
5. Halbmaier, K., J. Seikowski, ..., M. Bennati. 2016. High-resolution measurement of long-range distances in RNA: pulse EPR spectroscopy with TEMPO-labeled nucleotides. *Chem. Sci.* 7:3172–3180.
6. Becker, C. F., K. Lausecker, ..., M. Engelhard. 2005. Incorporation of spin-labelled amino acids into proteins. *Magn. Reson. Chem.* 43:S34–S39.
7. Stoller, S., G. Sicoli, ..., U. Diederichsen. 2011. TOPP: a novel nitroxide-labeled amino acid for EPR distance measurements. *Angew. Chem. Int. Ed.* 50:9743–9746.
8. Dastvan, R., B. E. Bode, ..., T. F. Prisner. 2010. Optimization of transversal relaxation of nitroxides for pulsed electron-electron double resonance spectroscopy in phospholipid membranes. *J. Phys. Chem. B.* 114:13507–13516.
9. Ghimire, H., R. M. McCarrick, ..., G. A. Lorigan. 2009. Significantly improved sensitivity of Q-band PELDOR/DEER experiments relative to X-band is observed in measuring the intercoil distance of a leucine zipper motif peptide (GCN4-LZ). *Biochemistry.* 48:5782–5784.
10. Schreier, S., J. C. Bozelli, Jr., ..., C. R. Nakaie. 2012. The spin label amino acid TOAC and its uses in studies of peptides: chemical, physicochemical, spectroscopic, and conformational aspects. *Biophys. Rev.* 4:45–66.
11. Fleissner, M. R., M. D. Bridges, ..., W. L. Hubbell. 2011. Structure and dynamics of a conformationally constrained nitroxide side chain and applications in EPR spectroscopy. *Proc. Natl. Acad. Sci. USA.* 108:16241–16246.
12. Toniolo, C., E. Valente, ..., J. L. Flippen-Anderson. 1995. Synthesis and conformational studies of peptides containing TOAC, a spin-labelled α , α -disubstituted glycine. *J. Pept. Sci.* 1:45–57.
13. Inbaraj, J. J., T. B. Cardon, ..., G. A. Lorigan. 2006. Determining the topology of integral membrane peptides using EPR spectroscopy. *J. Am. Chem. Soc.* 128:9549–9554.
14. Tkach, I., S. Pornsuwan, ..., M. Bennati. 2013. Orientation selection in distance measurements between nitroxide spin labels at 94 GHz EPR with variable dual frequency irradiation. *Phys. Chem. Chem. Phys.* 15:3433–3437.
15. Killian, J. A., I. Salemin, ..., D. V. Greathouse. 1996. Induction of nonbilayer structures in diacylphosphatidylcholine model membranes by transmembrane α -helical peptides: importance of hydrophobic mismatch and proposed role of tryptophans. *Biochemistry.* 35:1037–1045.
16. Matalon, E., I. Kaminker, ..., D. Goldfarb. 2013. Topology of the transmembrane peptide WALP23 in model membranes under negative mismatch conditions. *J. Phys. Chem. B.* 117:2280–2293.
17. Lueders, P., H. Jäger, ..., M. Yulikov. 2013. Distance measurements on orthogonally spin-labeled membrane spanning WALP23 polypeptides. *J. Phys. Chem. B.* 117:2061–2068.
18. Polyhach, Y., E. Bordignon, and G. Jeschke. 2011. Rotamer libraries of spin labelled cysteines for protein studies. *Phys. Chem. Chem. Phys.* 13:2356–2366.
19. Shen, Y., J. Maupetit, ..., P. Tufféry. 2014. Improved PEP-FOLD approach for peptide and miniprotein structure prediction. *J. Chem. Theory Comput.* 10:4745–4758.
20. Bode, B. E., D. Margraf, ..., O. Schiemann. 2007. Counting the monomers in nanometer-sized oligomers by pulsed electron-electron double resonance. *J. Am. Chem. Soc.* 129:6736–6745.
21. Junk, M. J., H. W. Spiess, and D. Hinderberger. 2011. DEER in biological multispin-systems: a case study on the fatty acid binding to human serum albumin. *J. Magn. Reson.* 210:210–217.
22. Dzikovski, B., D. Tipikin, and J. Freed. 2012. Conformational distributions and hydrogen bonding in gel and frozen lipid bilayers: a high frequency spin-label ESR study. *J. Phys. Chem. B.* 116:6694–6706.
23. Matalon, E., T. Huber, ..., D. Goldfarb. 2013. Gadolinium^{III} spin labels for high-sensitivity distance measurements in transmembrane helices. *Angew. Chem. Int.* 52:11831–11834.
24. de Planque, M. R. R., D. V. Greathouse, ..., J. A. Killian. 1998. Influence of lipid/peptide hydrophobic mismatch on the thickness of diacylphosphatidylcholine bilayers. A ²H NMR and ESR study using designed transmembrane α -helical peptides and gramicidin A. *Biochemistry.* 37:9333–9345.
25. Dzikovski, B. G., P. P. Borbat, and J. H. Freed. 2011. Channel and non-channel forms of spin-labeled gramicidin in membranes and their equilibria. *J. Phys. Chem. B.* 115:176–185.
26. Jeschke, G., V. Chechik, ..., H. Jung. 2006. DeerAnalysis2006—a comprehensive software package for analyzing pulsed ELDOR data. *Appl. Magn. Reson.* 30:473–498.

Biophysical Journal, Volume 111

Supplemental Information

Pulse EPR Measurements of Intramolecular Distances in a TOPP-Labeled Transmembrane Peptide in Lipids

Karin Halbmaier, Janine Wegner, Ulf Diederichsen, and Marina Bennati

Measurements of intramolecular distances in a TOPP-labeled transmembrane peptide in lipids by pulsed EPR spectroscopy

Supporting Information

Karin Halbmaier,¹ Janine Wegner,² Ulf Diederichsen,² and Marina Bennati^{1,2}

¹Electron Spin Resonance, Max Planck Institute for Biophysical Chemistry, Göttingen, Germany; ²Institute for Organic and Biomolecular Chemistry, Georg-August-University, Göttingen, Germany

Supplementary Materials and Methods

S1...Synthesis of labeled WALP24

S2...EPR experiments

S3...Molecular modeling of spin labeled WALP24

S4...Orientation selection in WALP24-TOPP experiments and their simulation

Supplementary Figures

Figure S1...Mass spectrometry

Figure S2...CD spectroscopy

Figure S3...Experimental PELDOR/DEER traces in methanol.

Figure S4...Model of WALP24-TOPP for simulation

Figure S5...Orientation selection experiment and simulation series 1

Figure S6...Orientation selection experiment and simulation series 2

Figure S7...Comparison of experiments from series 1 and series 2

Figure S8...PELDOR/DEER experiments on WALP24-MTSSL in DMPC for different peptide:lipid ratios

Figure S9...Echo decay data recorded on WALP24-MTSSL in MeOH and H54-DMPC

Figure S10... Experimental PELDOR/DEER traces recorded in deuterated lipids

Supplementary Materials and Methods

S1 Synthesis of labeled WALP24

Materials and general methods for peptide synthesis

Fmoc-Protected amino acids, coupling reagents and resins were obtained from *GL Biochem* (Shanghai, China), *Iris* (Marktredwitz, Germany), *Acros-Organics* (Geel, Belgium) and *Merck* (Darmstadt, Germany). The amino acid Fmoc-TOPP-OH was synthesized as mentioned in literature (1) The solvents in grades extra dry and puriss. absolute were purchased from *Acros-Organics* (Geel, Belgium), *Sigma Aldrich* (Schnelldorf, Germany) and *Fisher Scientific* (Loughborough, UK). MeOH for HPLC was purchased from commercially available sources and was used as supplied. Water for HPLC was purified using a water purification device from *Millipore* (Bedford, UK). Electrospray ionisation (ESI) mass spectra and high-resolution mass spectra (HR-MS-ESI) were recorded with a *Bruker* maXis spectrometer (Billerica, USA). Microwave assisted SPPS was performed with a *CEM* Discovery microwave instrument (Kamp-Lintfort, Germany). High-performance liquid chromatography was carried out on a *JASCO* instrument (Gross-Umstadt, Germany) using a *Macherey-Nagel* Nucleodur® RP C-18 analytical HPLC column (250 × 4.6 mm, 5 µm). HPLC runs were carried out using a linear gradient of 0.1% aq. TFA (solvent A) and MeOH/0.1% TFA (solvent B) in 30 min with a flow of 1 mL/min.

Loading of the first amino acid. The Fmoc-protected Rink Amide MBHA resin LL/ Fmoc-protected Rink Amide MBHA resin (1.0 eq) was swollen in a BD Discardit II syringe (*Becton Dickinson*, Fraga, Spain) in DMF for 2 h at room temperature and washed with NMP (5×) followed by microwave assisted Fmoc-deprotection with 20% piperidine in DMF (1: 50 °C, 25 W, 30 s; 2: 50 °C, 25 W, 3 min). Between the two deprotection steps the resin was washed with NMP (3×) and afterwards with NMP, DCM, DMF and NMP (10× each). Then a solution of Fmoc-Ala-OH (5.0 eq), 1 hydroxybenzotriazole (HOBt) (5.0 eq) and *N,N'*-diisopropylcarbodiimide (DIC) (5.0 eq) in DMF was added and the coupling was carried out by microwave irradiation (40 °C, 20 W, 10 min). Double coupling was performed. Between the coupling steps the resin was washed with NMP (3×) and after coupling subsequently with NMP, DCM, DMF, MeOH, Et₂O and DCM (5× each) and dried *in vacuo*. The loading density was estimated via UV analysis, followed by capping with 20% Ac₂O in NMP (1.5 mL) at room temperature for 10 min and washing with NMP, DCM, DMF and NMP (10 times each) (2).

General synthesis procedure for the TOPP labeled WALP24. The Fmoc-Ala-preloaded Rink Amide MBHA LL (0.05 µmol, 0.36 mmol/g, 1.00 eq) was swollen in DMF in a 2 mL BD Discardit II syringe for 2 h at room temperature followed by washing with NMP (5×). Each coupling cycle was started by microwave assisted double Fmoc-deprotection by adding 20% piperidine in DMF (1: 50 °C, 25 W, 30 s; 2: 50 °C, 25 W, 3 min) and washing between the deprotection steps with NMP (3×) and afterwards thoroughly with NMP, DCM, DMF and NMP (10 times each). The coupling mixture consisted of the respective amino acid (5.00 eq) in NMP (0.25 mL), a solution of HOBt/*O*-(benzotriazol-1-yl)-*N,N,N',N'*-tetramethyluronium hexafluorophosphate (HBTU) (5.00 eq/4.90 eq) in DMF (0.5 mL) and a 2 M solution of *N,N*-diisopropylethylamine (DIPEA) (10 eq) in NMP (0.25 mL). The mixture was added and the coupling was carried out by microwave irradiation (50 °C, 25 W, 10 min). Double coupling was performed and the resin was washed between the coupling steps with NMP (3×) and afterwards successively with NMP, DCM, DMF and NMP (10 times each). The amino acid Fmoc-TOPP-OH (2.00 eq) was coupled under inert gas in a flask with the coupling reagents 3-(diethoxyphosphoryloxy)-1,2,3-benzotriazin-4(3*H*)-one (DEPBT) (2.00 eq) and NaHCO₃ (2.00 eq) in dry THF (1.00 mL) at 0 °C for 4.5 h and room temperature for 30 min. After coupling the resin was washed with NMP, DCM, MeOH, Et₂O and DCM (10 times each). Double coupling and capping with 20% Ac₂O in NMP (1.5 mL) at room temperature for 10 min were performed followed by washing with NMP, DCM, DMF and NMP (10 times each). The following amino acids were coupled using standard conditions as mentioned above. Upon completion of the sequence the resin, was dried *in vacuo*.

General synthesis procedure for the cysteine mutated WALP24. The Fmoc-Ala-preloaded Rink Amide MBHA (1.00 µmol, 0.57 mmol/g, 1.00 eq) was swollen in DMF for 2 h at room temperature. The chain elongation was performed using a microwave assisted automatic peptide synthesizer Liberty™ (*CEM Corporation*, Matthews, NC). Each coupling cycle started with double Fmoc-deprotection with a 20% piperidine solution in NMP (1:50 °C, 25 W, 30 s; 2: 50 °C, 25 W, 3 min) followed by the coupling step. Each amino acid was activated by HOBt/HBTU (5.00 eq/4.90 eq) and DIPEA (10 eq). Double coupling was performed with microwave irradiation (75 °C, 25 W, 5 min). Cysteine was coupled at a lower temperature (50 °C, 25 W, 5 min). After synthesis the resin was dried *in vacuo*.

Cleavage and post-cleavage work up. The peptide cleavage from the resin and simultaneous deprotection of the protecting groups were performed at room temperature for 2 h in a mixture of

- TFA/H₂O/TIS (95/2.5/2.5, v/v/v) for the TOPP labeled peptide
- TFA/H₂O/EDT/TIS (94/2.5/2.5/1, v/v/v/v) for the cysteine mutated peptide.

After cleavage, the resulting solution was concentrated in a nitrogen stream and the addition of ice-cold Et₂O led to precipitation of the peptide. The resulting suspension was centrifuged at -5 °C followed by decanting the supernatant and washing of the peptide pellet with ice-cold Et₂O (3×). The raw peptide was dried *in vacuo*.

Reoxidation of the TOPP label. The raw peptide (1.00 eq) was dissolved in MeOH (100 μL for 2 mg), Cu(OAc)₂ (3.00 eq for each TOPP label) was added and the resulting mixture was stirred 2 h at room temperature followed by purification via HPLC.

Insertion of the MTSSL label. The raw cysteine mutated peptide (1.00 eq) was dissolved in MeOH (100 μL for 2 mg) and MTSSL (3.00 eq for each cysteine) was added. The resulting mixture was shaken over night at room temperature and then purified by HPLC.

TOPP labeled peptide. The following amino acids were used for the peptide synthesis: Fmoc-Trp(Boc)-OH, Fmoc-Lys(Boc)-OH, Fmoc-Ala-OH and Fmoc-Leu-OH. The desired peptide was obtained as a white solid after reoxidation of the TOPP label, purification by HPLC and lyophilisation.

Analytical data: HPLC (analytical, gradient 80 → 100% B in 30 min): $t_R = 23.05$ min. m/z (ESI) = 1023.5 [M+3H]³⁺, 1534.8 [M+2H]²⁺. m/z (HR-ESI-MS) = calculated: 1023.5777 [M+3H]³⁺, found: 1023.5781 [M+3H]³⁺ (Fig. S1).

MTSSL labeled peptide. The following amino acids were used for peptide synthesis: Fmoc-Trp(Boc)-OH, Fmoc-Lys(Boc)-OH, Fmoc-Cys(Trt)-OH, Fmoc-Ala-OH and Fmoc-Leu-OH. The desired peptide was obtained after labeling, purification by HPLC and lyophilisation as a white solid.

Analytical data: HPLC (analytical, gradient 80 → 100% B in 30 min): $t_R = 24.20$ min. m/z (ESI) = 753.7 [M+4H]⁴⁺, 1004.2 [M+3H]³⁺, 1505.8 [M+2H]²⁺. m/z (HR-ESI-MS) = calculated: 1004.2170 [M+3H]³⁺, found: 1004.2181 [M+3H]³⁺ (Fig. S1).

CD experiments. The peptide helical structure was investigated by CD spectroscopy in MeOH and in POPC or DMPC lipid vesicles. The measurement in solution was performed with peptide concentrations of 0.03 mg/mL for the TOPP labeled peptide and 0.1 mg/mL for the MTSSL labeled peptide. The experiments in lipids were performed with a peptide/lipid ratio of 1/30 in a 50 mM sodium phosphate buffer (pH 7.5) and peptide concentration of 0.03 mg/mL for the TOPP labeled peptide and 0.05 mg/mL of the MTSSL labeled peptide. For the preparation of the SUV, solutions of the peptide in MeOH and the lipid in CHCl₃ were mixed followed by removing of the solvents in a nitrogen stream. Then TFE was added and also removed in a nitrogen stream. The resulting lipid film was dried overnight *in vacuo* at 40 °C. The buffer was added and the film swollen for 30 min at room temperature followed by vortexing the mixture for 1 min at 5 min intervals (3×). To form SUV the mixture was treated with ultrasound sonifier sonoplus HD2076 (Bandelin, Berlin, Germany; 30 min, Cycle 4, 60% power). CD spectra are displayed in Fig. S2.

S2 EPR experiments

Determination of labeling efficiency. CW-EPR spectroscopy at X-band frequencies was employed to characterize the label efficiency of WALP24-MTSSL samples. Room temperature experiments were performed in a Bruker Elexsys E500 spectrometer equipped with a Bruker super-high Q resonator ER4122SHQE. Glass capillaries of 1 mm inner diameter (ID) were filled with a sample volume 20 μl. Spin concentrations were calculated by doubly integrating the CW-EPR spectrum and comparing the intensity with a calibration curve recorded with 4-hydroxy-TEMPO at concentrations between 5 and 100 μM as well as with the nominal WALP24-MTSSL concentration determined by UV absorbance of the tryptophans. Labeling efficiencies around 80-90 % were determined for different batches. As the determination of WALP24-TOPP's concentration is potentially compromised by the interference of TOPP's absorption spectrum in the WALP24 with the tryptophans, the labeling efficiency can be alternatively estimated from a comparison of the modulation depths of experiments on WALP24-MTSSL and WALP24-TOPP. The software DeerAnalysis offers a tool to calibrate experimental modulation depths to a known labeling efficiency following the relation between the average number of spins per molecule

$\langle n \rangle$ ($n = 2 = 100\%$ labeling efficiency), the modulation depth parameter λ (dependence on excitation position, length, and flip angle of the pump pulse) and the total modulation depth Δ : $\Delta = 1 - [\lambda(\langle n \rangle - 1)]$.⁽³⁾ A comparison of the modulation depths observed in the PELDOR/DEER experiments on WALP24 in MeOH, suggests a labeling efficiency of 65-75 % for WALP24-TOPP. However, we note that this is an estimation as no modulation depth calibration was performed.

labeling efficiency WALP24-MTSSL determination via cw-EPR (experimental modulation depth = 28 %)	labeling efficiency WALP24-TOPP estimation (experimental modulation depth = 16.5 %)
100 % (2 spins)	77.5 % (1.55 spins)
80 % (1.6 spins)	66.5 % (1.33 spins)

Despite the results obtained in the MS spectra, the labeling efficiency of WALP24-TOPP was lower than for WALP24-MTSSL. It seems that the TOPP label is more labile towards reduction, as the spin concentration in the sample was decreasing during the sample preparation procedure.

EPR sample preparation. For experiments in solution, WALP24-TOPP and WALP24-MTSSL were dissolved in MeOH containing 20 % glycerol yielding a spin concentration of 40 μM . EPR samples of WALP24-TOPP and WALP24-MTSSL in deuterated phospholipid multilamellar vesicles (MLV's) were prepared by mixing stock solutions of the peptide in methanol and the deuterated phospholipid (*Avanti*) in chloroform, yielding a spin concentration of 40 μM (20 μM peptide if labeling efficiency = 100 %) in the final sample volume and a spin:phospholipid molar ratio of 1:3000 (peptide:phospholipid = 1:6000 if labeling efficiency = 100 %). Solvents were removed under nitrogen gas stream followed by 3-4 h vacuum drying. Tris-HCl buffer (20 mM, pH = 7.4) was added to the peptide lipid film and the resulting suspension was mixed on a vortex mixer for 2 min above the lipids transition temperature. Three freeze-thaw cycles were employed to increase the homogeneity of the vesicles. After 30 min of incubation $\sim 50 \mu\text{L}$ were mounted into an EPR tube (3 mm o.d., 2mm i.d) and rapidly frozen in liquid nitrogen. Additionally samples of WALP24-MTSSL in DMPC with different peptide:lipid ratios were prepared (Fig. S8) by mixing stock solutions of the peptide in methanol and the phospholipid (*Avanti*) in dichloromethane, yielding a peptide concentration of 30 μM in the final sample volume and the desired peptide:phospholipid molar ratio. Tris-HCl buffer (20 mM, pH = 7.4) was added to the peptide lipid film and the resulting suspension was mixed on a vortex mixer for 2 min above the lipids transition temperature. After incubation 15 μL were transferred into an EPR tube (2 mm o.d., 1.5 mm i.d) and rapidly frozen in liquid nitrogen. For comparison 15 μL WALP-MTSSL in MeOH containing 20 % glycerol in an EPR tube (2 mm o.d., 1.5 mm i.d) were prepared.

PELDOR/DEER and echo decay experiments. EPR distance measurements were performed using a commercial Bruker ElexSys E580 pulse X/Q-band spectrometer equipped with a pulsed 170 W Q-band TWT-amplifier (Model 187Ka, Applied Systems Engineering Inc.). All PELDOR/DEER experiments were performed using the four-pulse DEER sequence. The experimental temperature of 50 K was achieved with a continuous flow cryostat (CF95550, Oxford Instruments). Experiments on WALP24 in EPR tubes of 3 mm outer diameter (2 mm inner diameter) were performed with the Bruker ER5107QT-II resonator giving a typical π -pulse length of 16-18 ns when frequency was tuned in the dip center of the microwave resonator and 26-28 ns when shifted 90 MHz. The pumping frequency was set in the resonator dip center and at the maximum of the nitroxide's EPR spectrum, detection frequency was shifted 90 MHz lower. Time delay between the first two pulses in the sequence was set to 400 ns. The dipolar evolution time T (spacing between the first Hahn echo and third detection pulses) was set to 1.9 μs , the last 400 ns of the traces usually contained artifacts and were not considered. Typical acquisition times were on the order 10 to 15 h. Experiments on WALP24-MTSSL in MeOH and DMPC at different peptide:lipid ratios were conducted with smaller sample volumes. For tubes of 1.5 mm outer diameter (1 mm inner diameter) the EN5107D2 Bruker resonator was employed. This resonator delivered a typical π pulse length of 12 ns at the center of the dip and 20-24 ns when the frequency is shifted 90 MHz. The pumping frequency was set in the resonator dip center and at the maximum of the nitroxide's EPR spectrum, while detection frequency shifted 90 MHz lower. Time-delay between the first two pulses in the sequence was set to 300 ns. The dipolar evolution time T (spacing between the first Hahn echo and third detection pulses) was set to 1.4 μs and 0.7 μs for the ratio of 1:250, the last 200 ns of the traces usually contained artifacts and were not considered. Acquisition times were on the order 20 h. For data analysis, dipolar traces were background corrected using either a mono-exponential or a second-order polynomial function. Distance distributions were obtained with the program DeerAnalysis⁽³⁾, using a fitting procedure based on Tikhonov regularization. The echo decay data on this sample set were recorded with the two-pulse Hahn echo sequence with a systematic increase of the spacing between the two pulses from 300-16636 ns. Detection was set to the maximum of the EPR line.

S3 Molecular modeling of spin labeled WALP24

For the MTSSL containing peptide, an energy minimization of the peptide structure containing the cysteine mutation was performed using PEP-FOLD (5) with subsequent attachment of possible rotamers of MTSSL calculated using MMM (6). For WALP24-TOPP, an optimized WALP24 peptide structure was computed by inserting a tyrosine at the label position to account for possible aromatic π -interaction by the TOPP label. In the geometry optimized structure the tyrosine was subsequently replaced by TOPP, with the TOPP structure as minimized earlier (1).

S4 Orientation selection in WALP24-TOPP experiments and simulation

To investigate the orientation selection expected for the TOPP label a series of experiments and simulations were performed. In order to evaluate the dependence of the dipolar frequency on the experimental set up, experiments were performed with a constant spectral position for pump frequency while varying the frequency separation and therefore only the detection position (series 1 and 2, Fig. S5 and S6). Simulations were conducted using a home written program that takes into account orientation selection in PELDOR experiments (4). Experimental parameters (pulse lengths, frequency separation, EPR detection frequency, nitroxide EPR parameters) were considered in the simulation. Relative orientation of the two TOPP labels was extracted from the minimized WALP24-TOPP structure and the experimental distance. To take into account the rotational freedom of the TOPP label around its two single bonds, Φ_1 and Φ_2 (defined in Fig.1, main text), the simulations were conducted by rotating around the x-axis of the g- and A-tensor which is parallel to the respective single bonds (Fig. S4). A rotation of $\pm 25^\circ$ for $\Phi_1 + \Phi_2$ to average orientation selection (as observed in our earlier study(4)) was used to examine the difference in the orientation selectivity as compared to the case $\pm 0^\circ$. Interestingly, there is no distinguishable difference between these two cases (Fig. S5 and S6). The results illustrate that orientation selection is not observed when broadband excitation is applied.

Supplementary Figures

Figure S1: Mass spectra of WALP24.

Up: ESI mass spectrum of the TOPP labeled peptide including the HR-MS-ESI of the $[M+3H]^{3+}$ -species as inset. Down: ESI mass spectrum of the MTSSL labeled peptide including the HR-MS-ESI of the $[M+3H]^{3+}$ -species as inset.

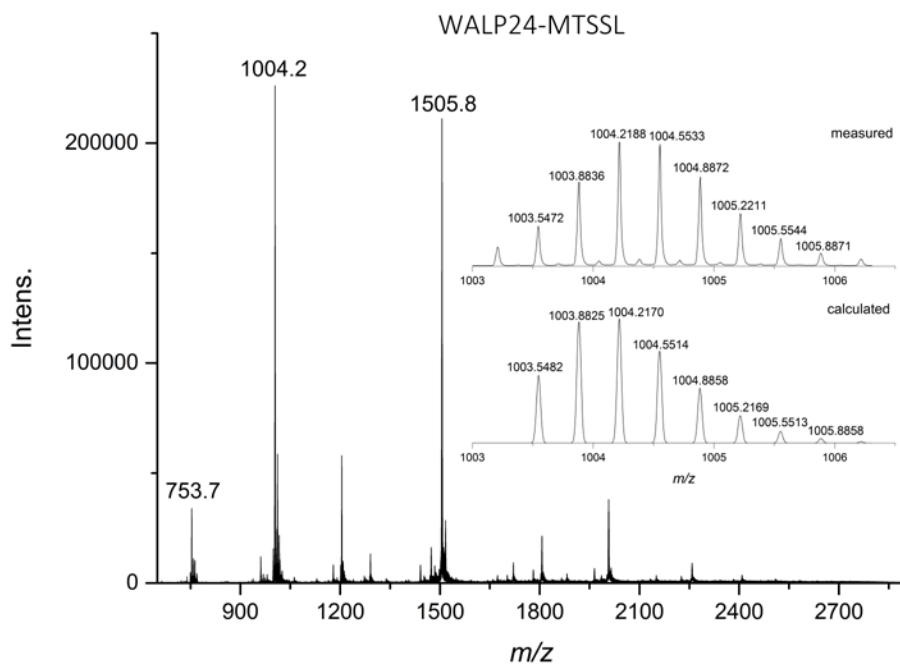
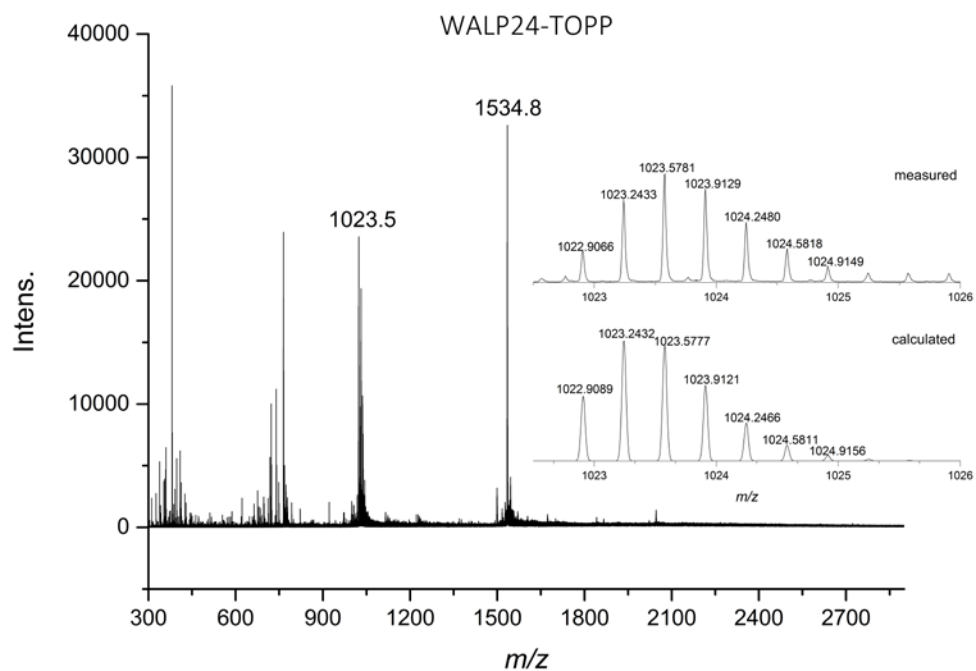


Figure S2: CD spectra of WALP24.

Two characteristic minima at 208 nm and 222 nm indicate α -helical structure. Left: WALP24-TOPP measured in MeOH (black line) and in lipids (colored lines). right; WALP24-MTSSL measured in MeOH (black line) and in lipids (colored lines).

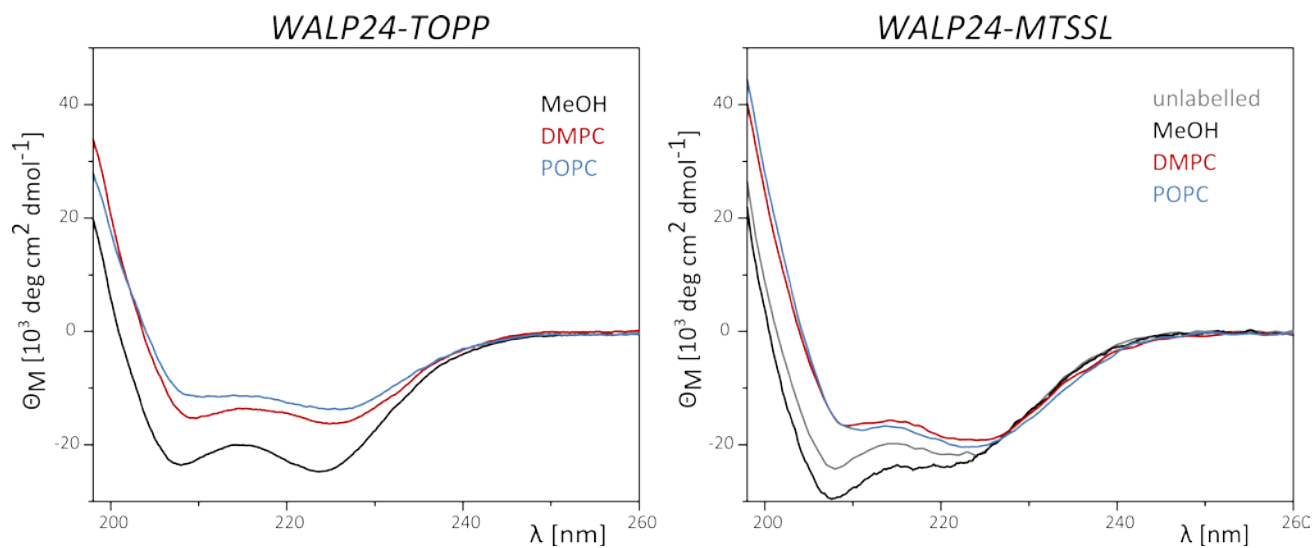


Figure S3: Experimental PELDOR/DEER traces in methanol

A: Experimental time traces of WALP24-TOPP (left) and WALP24-MTSSL (right) recorded in methanol solution.

B: Comparison of distance distribution for WALP24-MTSSL in methanol obtained with Tikhonov regularization using DeerAnalysis (3) (left) with Fourier transformation of the data (right). To test whether the peaks in distance distribution delivered by Tikhonov regularization were real, we have calculated the FT spectrum for each peak and compared it to the FT spectrum of the data. The experimental FT spectrum is well consistent with the sum of at least two distance distributions as given by DeerAnalysis (red and blue curves).

C: Estimation of the uncertainty of the peak distance in the PELDOR traces of WALP24-TOPP in methanol. Illustrated is the expected, simulated (red lines, right), dipolar oscillation as a function of a shift in the peak distance up to ± 0.1 nm (left). A Gaussian distance distribution of half width $\Delta r = \pm 0.2$ nm was considered for the peak distance (red lines, left) with an added noise of the size of the experimental data. It becomes clear that, for the given S/N, a shift of ≥ 0.5 Å in the peak distance is detectable.

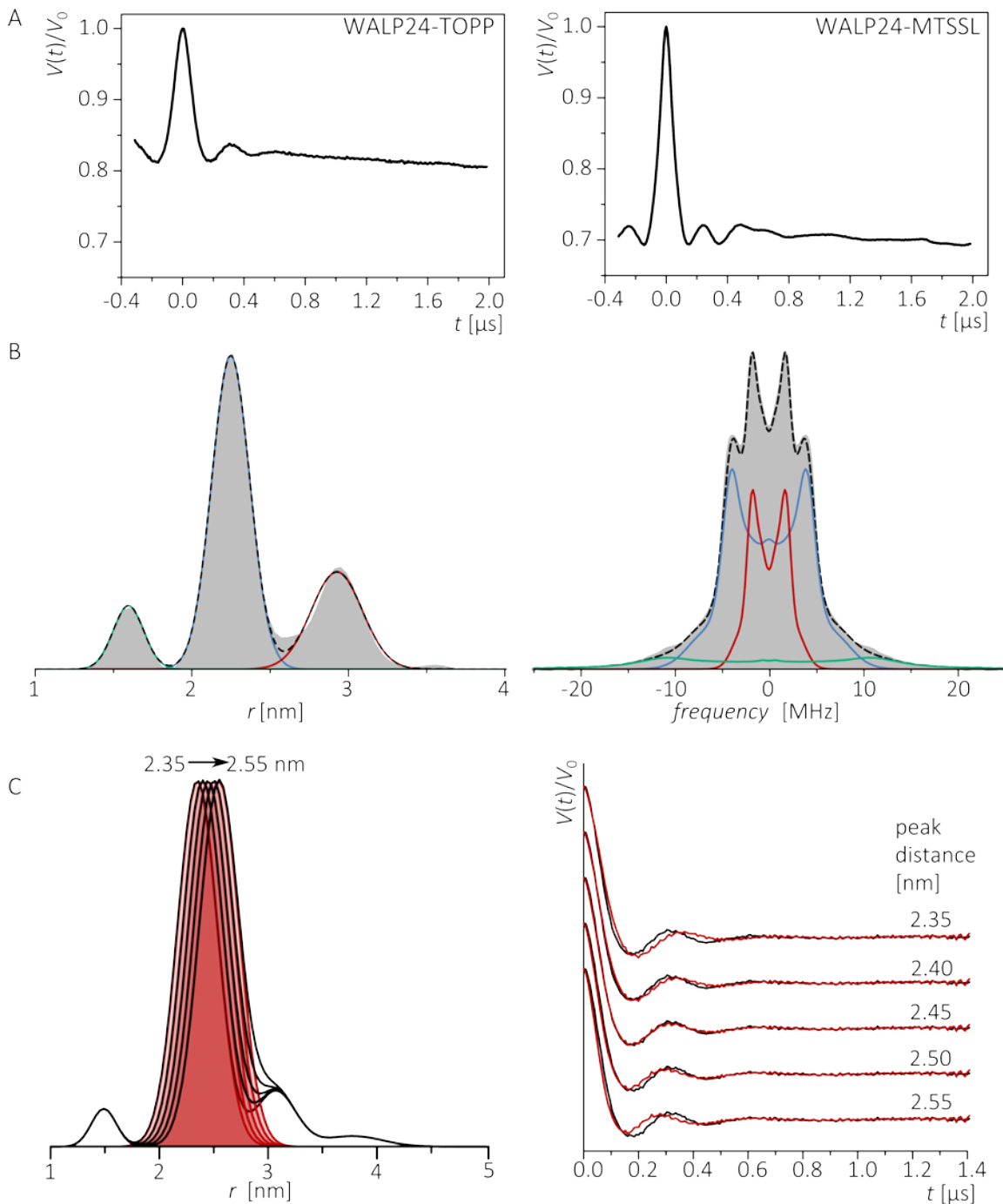


Figure S4: Model of WALP24-TOPP for simulation

Chemical structure of TOPP and orientation of the magnetic g- and A-tensor, which are collinear in the nitroxide radical (left), g- and A-tensor as published in (4). Pymol Model of TOPP attached to minimized WALP24-Y (X = Y. TOPP label at position 5 (label 2) and position 20 (label 1) rotated $\pm 25^\circ$ around one of the single bonds illustrating the rotation around the g-tensors x-axis. Methyl-groups and oxygen are hidden for simplicity.

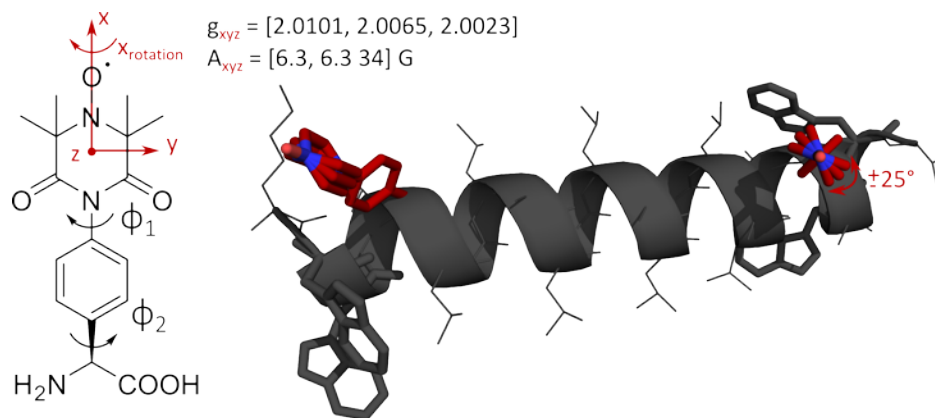


Figure S5: Orientation selection experiment and simulation series 1

A: Experimental set up series 1: experimental ESE (black line), and pulses according to the experimental set up (colored) with the pump pulse applied at the maximum of the EPR spectrum. Frequency separation between pump and detection was varied from 70 MHz to 130 MHz. Pulse lengths were 12 and 18-28 ns for pumping and detection respectively.

B: Fits obtained by Tikhonov regularization performed with DeerAnalysis (left, colored lines) of the experimental time traces (left, black lines), their Fourier transformations (middle) and corresponding distance distributions (right). Experimental time traces and distance distributions show no dependence on the experimental set up.

C: Orientation selective experiments and simulations series 1. Top: experimental (left) and simulated time traces (for rotation around the x-axis of 0° (middle) and $\pm 25^\circ$ (right)) for the four set ups of series 1. Bottom: Time traces and corresponding Fourier transformations (inset). The black line, plotted on top of orientation selective simulations (middle, right), displays a simulation with full excitation of the nitroxide's EPR line for comparison, but no significant differences are observed. Minor differences between the PELDOR/DEER signals simulated with experimental conditions or full excitation of the EPR line are not resolved in the experiment (Fig. S7).

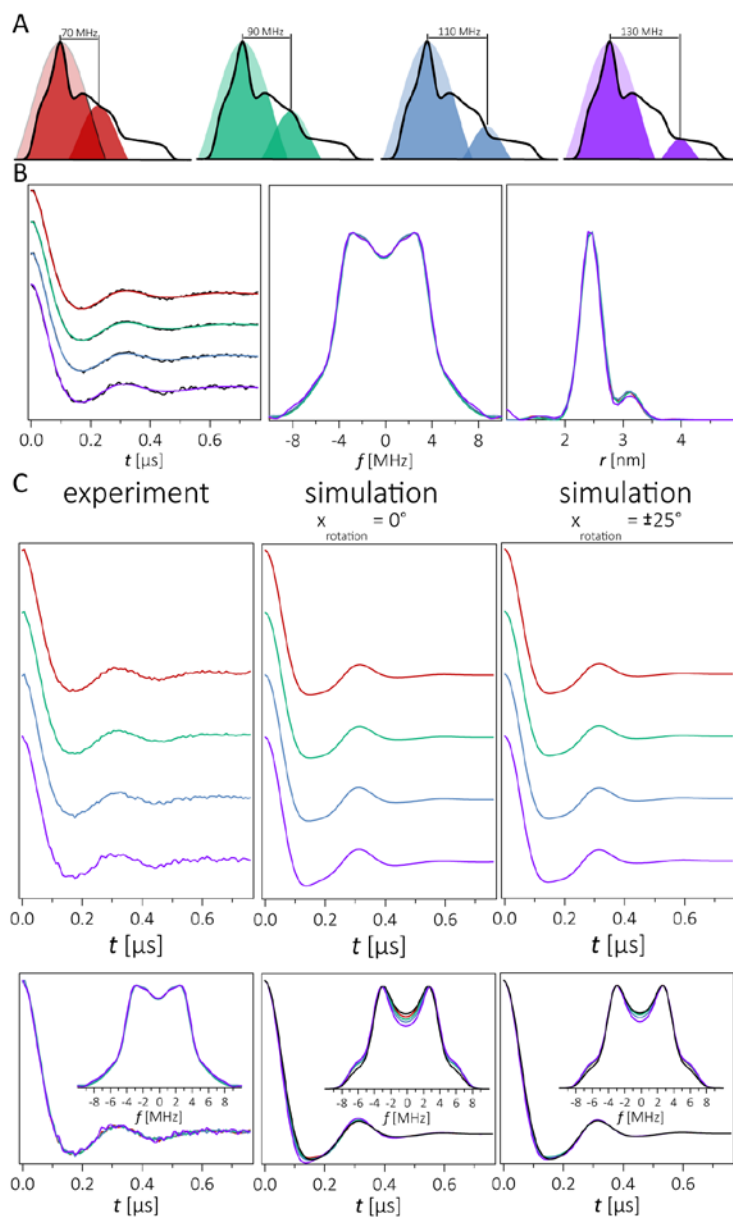


Figure S6: Orientation selection experiment and simulation series 2

A: Experimental set up series 2: experimental ESE (black line), and pulses according to the experimental set up (colored) with the pump pulse applied 10 G below the maximum of the EPR spectrum. Frequency separation between pump and detection was varied from 70 MHz to 130 MHz. Pulse lengths were 12 and 18-28 ns for pumping and detection respectively.

B: Fits obtained by Tikhonov regularization performed with DeerAnalysis (left, colored lines) of the experimental time traces (left, black lines), their Fourier transformations (middle) and corresponding distance distributions (right). Experimental time traces and distance distributions show no dependence on the experimental set up.

C: Orientation selective experiments (left) simulations series 2. Top: experimental (left) and simulated time traces (for rotation around the x-axis of 0° (middle) and $\pm 25^\circ$ (right)) for the four set ups of series 2. Bottom: Time traces and corresponding Fourier transformations (inset). The black line, plotted on top of orientation selective simulations (middle, right), displays a simulation with full excitation of the nitroxide's EPR line for comparison, but no differences are observed. The results best illustrate the absence of orientation selective effects with broadband excitation.

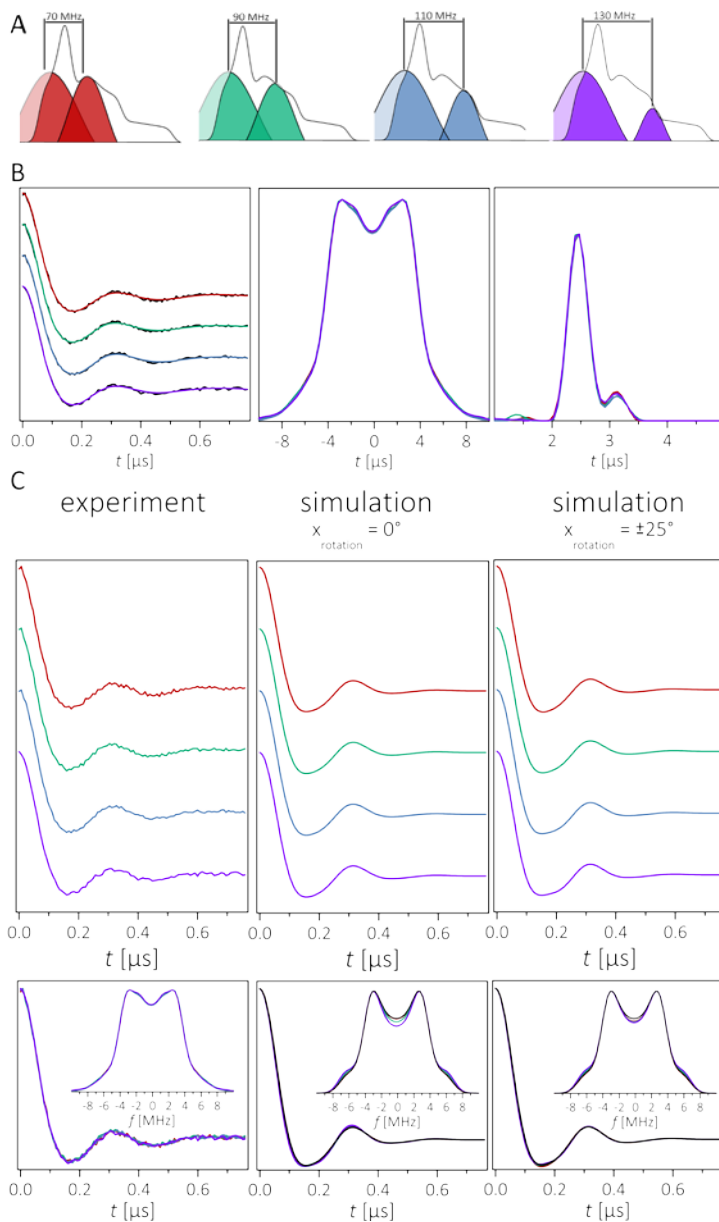


Figure S7: Comparison of experiments from series 1 and series 2

A: Experimental set up: experimental ESE (black line), and pulses according to the experimental set up. Frequency separation between pump and detection was 90 MHz. Pulse lengths were 12 and 18 ns for pumping and detection respectively.

B: Orientation selective simulations series for PELDOR/DEER experiments with 90 MHz frequency separation and pump position either at the maximum of the EPR line (black) or set 10 G lower (gray). Only subtle differences are observed comparing both simulations. A simulation with full excitation of the EPR line is shown in red.

C: Fits of the time traces with Tikhonov regularization (lines, left) of the experimental time traces (dots, left), their Fourier transformations (middle) and corresponding distance distributions (right). Experimental time traces and distance distributions show no dependence on the experimental set up. The subtle differences in simulations for both set ups are not resolved in the experiments. The set up employing the pump pulse at the maximum of the EPR line was chosen for all experiments as it delivers higher modulation depths and higher signal-to-noise ratios.

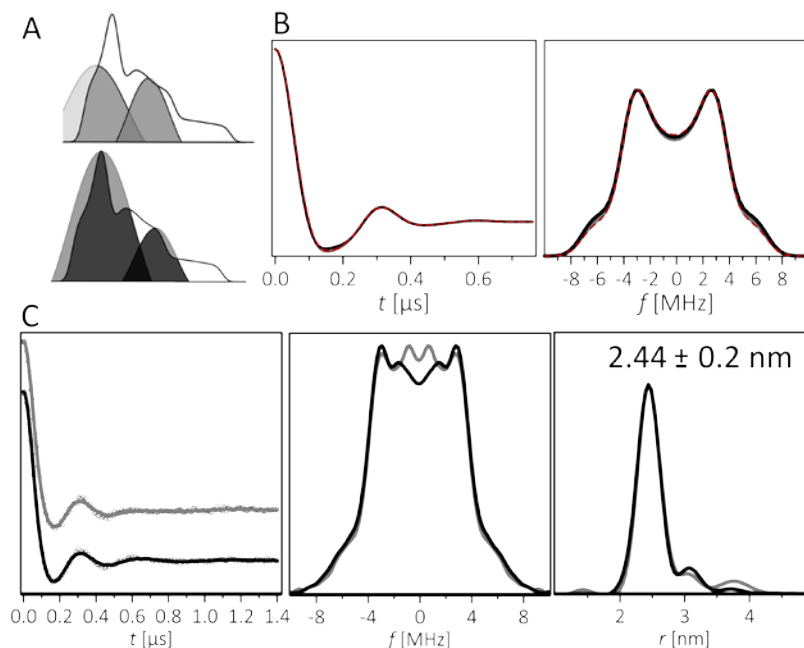


Figure S8: PELDOR/DEER experiments on WALP24-MTSSL in DMPC (protonated) for different peptide-to-lipid ratios.

Experimental PELDOR/DEER traces (left), dipolar traces after background subtraction and their total modulation depth Δ (definition in S2) observed in the experiments (right). Modulation depth for the 1:250 peptide-to-lipid ratio appears much more reduced than in the other samples. However we note that the Δ value in this sample has a larger uncertainty due to the reduced length of the trace (left) and the subsequent difficulty of performing a background subtraction. Nevertheless, a clear trend in increasing echo decay is observed from 1:250 -> 1:3000 peptide-to-lipid ratio, as reported in the main text.

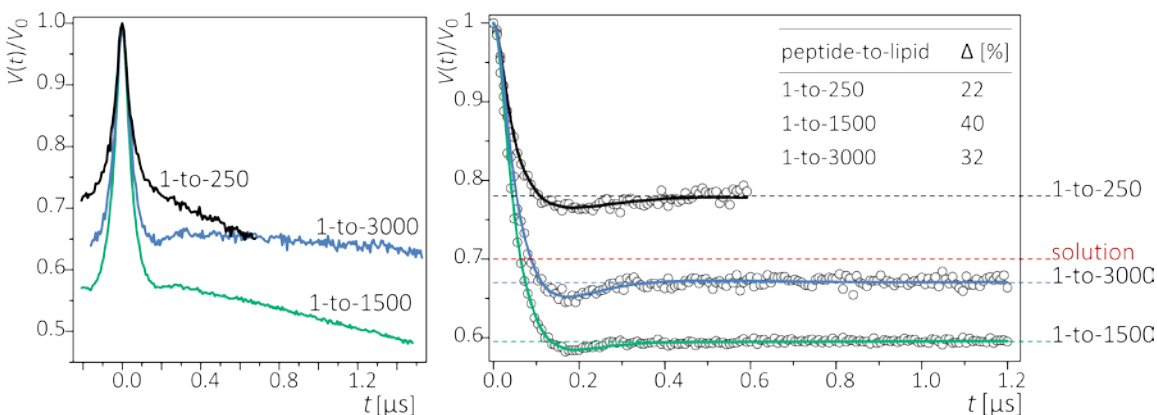


Figure S9: Representative two-pulse echo decay data at Q band recorded on WALP24-MTSSL in MeOH and H54-DMPC.

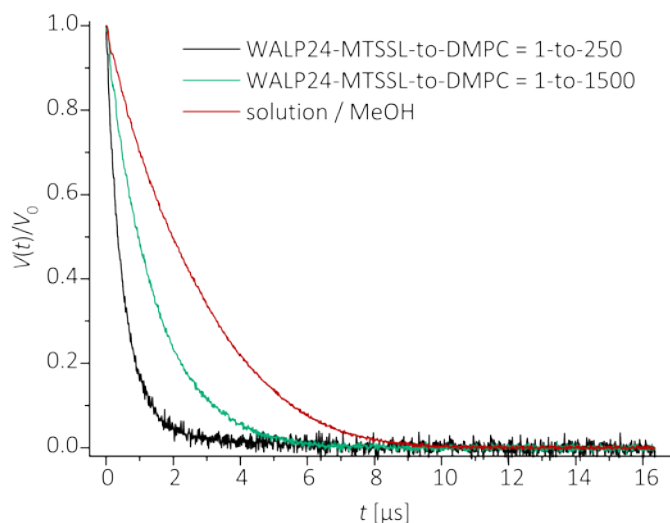
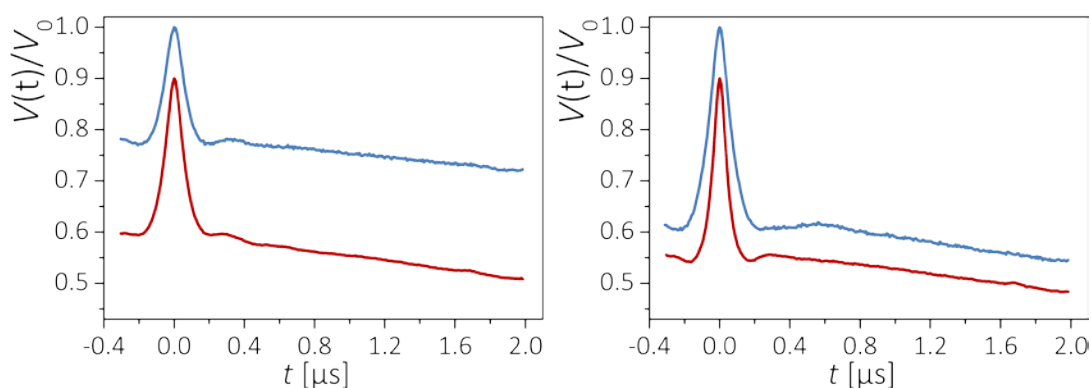


Figure S10: Experimental PELDOR/DEER traces recorded on WALP24-TOPP (left) WALP24-MTSSL (right) in deuterated lipids D54-DMPC (red) and D31-POPC (blue) prior background subtraction.



REFERENCES

1. Stoller, S., G. Sicoli, T. Y. Baranova, M. Bennati, and U. Diederichsen. 2011. TOPP: a novel nitroxide-labeled amino acid for EPR distance measurements. *Angewandte Chemie* 50:9743-9746.
2. Gude, M., J. Ryf, and P. D. White. 2002. An accurate method for the quantitation of Fmoc-derivatized solid phase supports. *Letters in Peptide Science* 9:203-206.
3. Jeschke, G., V. Chechik, P. Ionita, A. Godt, H. Zimmermann, J. Banham, C. R. Timmel, D. Hilger, and H. Jung. 2006. DeerAnalysis2006—a comprehensive software package for analyzing pulsed ELDOR data. *Applied Magnetic Resonance* 30:473-498.
4. Tkach, I., S. Pornsuwan, C. Hobartner, F. Wachowius, S. T. Sigurdsson, T. Y. Baranova, U. Diederichsen, G. Sicoli, and M. Bennati. 2013. Orientation selection in distance measurements between nitroxide spin labels at 94 GHz EPR with variable dual frequency irradiation. *Physical chemistry chemical physics : PCCP* 15:3433-3437.
5. Shen, Y., J. Maupetit, P. Derreumaux, and P. Tuffery. 2014. Improved PEP-FOLD Approach for Peptide and Mini-protein Structure Prediction. *Journal of chemical theory and computation* 10:4745-4758.
6. Polyhach, Y., E. Bordignon, and G. Jeschke. 2011. Rotamer libraries of spin labelled cysteines for protein studies. *Physical chemistry chemical physics : PCCP* 13:2356-2366.
7. Bode, B. E., D. Margraf, J. Plackmeyer, G. Dürner, T. F. Prisner, and O. Schiemann. 2007. Counting the Monomers in Nanometer-Sized Oligomers by Pulsed Electron–Electron Double Resonance. *Journal of the American Chemical Society* 129:6736-6745.
8. Dastvan, R., B. E. Bode, M. P. R. Karuppiyah, A. Marko, S. Lyubenova, H. Schwalbe, and T. F. Prisner. 2010. Optimization of Transversal Relaxation of Nitroxides for Pulsed Electron–Electron Double Resonance Spectroscopy in Phospholipid Membranes. *The Journal of Physical Chemistry B* 114:13507-13516.